Dalton Transactions

ROYAL SOCIETY OF CHEMISTRY

COMMUNICATION

View Article Online
View Journal | View Issue

Check for updates

Cite this: *Dalton Trans.*, 2024, **53**, 17777

Received 30th September 2024,
Accepted 24th October 2024

DOI: 10.1039/d4dt02766c

rsc.li/dalton

Synthesis and relaxivity of gadolinium-based DOTAGA conjugated 3-phosphoglycerate†

Andrew R. Brotherton, Shifa Noor Mohamed and Thomas J. Meade *

The synthesis and characterization of a gadolinium-based contrast agent conjugated to 3-phosphoglycerate (*Gd-3PG*) are reported. The synthetic steps are optimized to incorporate a selective deprotection strategy for a primary *tert*-butyl dimethyl silyl (TBS) hydroxyl over a secondary one. The relaxivity of *Gd-3PG* shows characteristic improvement, likely due to secondary sphere effects and/or an increase in molecular weight (5.39 ± 0.14 mM^{-1} s^{-1} at 1.4 T and 37 °C). Michaelis–Menten enzymatic kinetics was measured on the modified 3PG-arm and it showed similar activity to the native 3PG metabolite, K_m = 240 ± 30 μM. This agent and future versions of this type of GBCA, which are conjugated to glycolytic metabolites, were designed to monitor *in vivo* allosteric regulatory events in glycolytic processes.

Open Access Article. Published on 25 October 2024. Downloaded on 4/21/2026 11:49:17 AM.
This article is licensed under a Creative Commons Attribution-NonCommercial 3.0 Unported Licence.

Introduction

Gadolinium-based contrast agents (GBCAs) are routinely used in the clinic for magnetic resonance imaging (MRI) and for molecular imaging in important discovery experiments.[1–4] Conjugation or binding of GBCAs to a protein enhances the relaxivity (r_1) by slowing down the rotational correlation time (τ_r), commonly known as a τ_r boost.[5] The GBCAs are likewise investigated using electron nuclear double resonance (ENDOR) as alternatives for measuring the amino acid distances of proteins *in situ*,[6] where typical crystallization techniques have difficulties elucidating the dynamic conformations.

Biomolecular chemistry is challenging to visualize *in vivo*, especially with its unique allosteric regulatory effects. For example, highly energetic metabolites like 1,3-bisphosphoglycerate (1,3-BPG) have been shown to non-enzymatically and covalently tag exposed lysine residues on nearby proteins in a metabolic regulatory process.[7] Our work focuses on the synthesis and characterization of such an agent by conjugating 3-phosphoglycerate (3PG) to a GBCA. ***Gd-3PG*** shows an enhanced r_1, most likely attributed to secondary sphere effects or an increase in molecular weight from the 3PG-arm.[8] The 3PG-arm had a similar Michaelis–Menten constant (K_m) to that of reported 3PG in the phosphorylation to 1,3-BPG by phosphoglycerate kinase (PGK).[9]

Experimental

General methods

Unless otherwise noted, all synthetic manipulations were performed under a dry nitrogen atmosphere using standard Schlenk techniques. Solvents were still dried using Glass Contour columns or over-activated molecular sieves (4 angstroms). Reactions were monitored by TLC using precoated plastic plates (0.20 mm silica gel 60, UV_{254}, Macherey-Nagel GmbH & Co., Duren Germany). Spots were visualized using potassium permanganate stain, Dragendorff stain, CAM stain, or UV active methods. ^{1}H NMR and proton-decoupled ^{13}C NMR spectra were recorded on a Bruker Avance III spectrometer (499.37 MHz for ^{1}H, 125.58 MHz for ^{13}C, and 150 MHz for ^{31}P) and were processed using Bruker TOPSPIN 2.1 software. ^{1}H, ^{13}C, and ^{31}P chemical shifts are reported as δ values in parts per million downfield from tetramethylsilane (TMS) or external triethyl phosphate. High-resolution mass spectrometry (HRMS) was performed using an Agilent 6210 time-of-flight (TOF) LC/MS instrument using electrospray ionization (ESI). Deuterated solvents were purchased from Cambridge Isotope Labs or Sigma-Aldrich. For high-performance liquid chromatography, an Agilent 1160/1260 DAD was used for traces, with ESI for ionization and 6120 Quadrupole LC/MS for detection. The analytical column was a Synergi 4 μm Polar-RP 80 Å, 4.6 × 150 mm column, and the semipreparative column was a Synergi 4 μm Polar-RP 80 Å 21.2 × 150 mm column.

Departments of Chemistry, Molecular Biosciences, Neurobiology, and Radiology, Northwestern University, 2145 Sheridan Road, Evanston, Illinois 60208-3113, USA. E-mail: tmeade@northwestern.edu

† Electronic supplementary information (ESI) available. See DOI: https://doi.org/10.1039/d4dt02766c

Open Access Article. Published on 25 October 2024. Downloaded on 4/21/2026 11:49:17 AM. This article is licensed under a Creative Commons Attribution-NonCommercial 3.0 Unported Licence.

Synthesis

Precursors methyl (*R*)-2,3-dihydroxypropanoate (2) and *tert*-butyl (*S*)-2,5-dihydroxypentanoate (8) were synthesized using previous literature procedures.[10–12]

Methyl (*R*)-2,3-bis((*tert*-butyldimethylsilyl)oxy)propanoate (3). **2** (0.7990 g, 6.65 mmol) was dissolved in DMF (14 mL) and then imidazole (1.1784 g, 17.3 mmol) and TBSCl (2.3012 g, 15.2 mmol) were added sequentially. The reaction was allowed to stir at rt overnight. The reaction was diluted with water (20 mL), extracted with EtAc (3 × 100 mL), and concentrated before purification by flash column chromatography (20% DCM in Hex, r_f = 0.2) to afford a clear oil (2.3561 g, 92% yield). **^{1}H-NMR** (500 MHz, $CDCl_3$, δ): 4.26 (dd, 1H), 3.76 (dd, 2H), 3.70 (s, 3H), 0.88 (s, 9H), 0.86 (s, 9H), 0.07 (s, 3H), 0.06 (s, 3H), 0.03 (m, 6H). **^{13}C-NMR** (125 MHz, $CDCl_3$, δ): 172.48, 74.01, 65.96, 51.76, 25.83, 25.72, 18.36, 18.31, −5.06, −5.08, −5.38, −5.46.

Methyl (*R*)-2-((*tert*-butyldimethylsilyl)oxy)-3-hydroxypropanoate (4). **3** (7.0814 g, 20.3 mmol) was dissolved in a mixture of acetone (35.4 mL), acetic acid (77.9 mL), and water (42.5 mL) and stirred for 24 h at rt. The solution was then slowly quenched on ice (0 °C) with solid $NaHCO_3$, extracted with DCM (4 × 200 mL), dried over Na_2SO_4, and concentrated. The remaining oil was purified by flash column chromatography (10% EtAc in Hex, r_f = 0.15) to afford a clear oil (3.2473 g, 68% yield). **^{1}H-NMR** (500 MHz, $CDCl_3$, δ): 4.29 (dd, 1H), 3.78 (m, 2H), 3.73 (s, 3H), 2.14 (t, 1H), 0.90 (s, 9H), 0.12 (s, 3H), 0.07 (s, 3H). **^{13}C-NMR** (125 MHz, $CDCl_3$, δ): 172.25, 72.77, 65.04, 52.09, 25.70, 18.33, −4.89, −5.39. **HRMS ESI-MS**: 257.118 *m*/*z* $[M + H]^+$ calculated for $C_{10}H_{22}O_4Si$, 257.126 found.

Methyl (2*R*)-3-((*tert*-butoxy(diisopropylamino)phosphaneyl)oxy)-2-((*tert*-butyldi methylsilyl)oxy)propanoate (5). Under argon, **4** (0.5456 g, 2.33 mmol) was dissolved in ACN (4.5 mL). Diisopropylammonium tetrazolide salt (0.7030 g, 4.09 mmol) and *tert*-butyl tetraisopropylphosphorodiamidite (0.9011 g, 2.96 mmol) were added rapidly and sequentially. The solution was stirred at rt for 3 h and concentrated. The residue was resuspended in ether, vacuum filtered, and concentrated. The clear oil was purified on a plug of deactivated silica (10% EtAc in Hex with 1% TEA, r_f = 0.85). The silica was deactivated by passing the mobile phase through several plug volumes. A clear oil was collected (1.0189 g, 95% yield). **^{1}H-NMR** (500 MHz, $CDCl_3$, δ): 4.33 (dd, 1H), 3.78 (m, 0.5H), 3.69 (m, 3/1H), 3.56 (m, 0.5H), 1.31 (d, 9H), 1.13 (m, 12H), 0.88 (d, 9H), 0.07 (s, 3H), 0.06 (d, 3H). **^{13}C-NMR** (125 MHz, $CDCl_3$, δ): 172.42, 74.86, 74.81, 73.02, 72.96, 65.03, 64.92, 51.77, 43.02, 42.92, 30.86, 30.79, 25.71, 24.52, 24.20, 18.31, −5.06, −5.11. **^{31}P-NMR** (150 MHz, $CDCl_3$, δ): 138.77, 138.26. **HRMS ESI-MS**: 438.280 *m*/*z* $[M + H]^+$ calculated for $C_{20}H_{44}NO_5PSi$, 438.341 found.

***tert*-Butyl (2*S*)-5-((*tert*-butoxy((*R*)-2-((*tert*-butyldimethylsilyl)oxy)-3-methoxy-3-oxopropoxy)phosphoryl)oxy)-2-hydroxypentanoate (9).** Under argon, **5** (0.9333 g, 2.14 mmol) was dissolved in ACN (4 ml), and the temperature was adjusted to −41 °C. A solution of **8** (0.4060 g, 2.14 mmol) in ACN (3 mL) and 1*H*-tetrazole (6.75 mL of a 0.4 M solution in ACN, 2.70 mmol) were added. The solution was allowed to slowly warm while in an ice bath. TLC monitored at 5 h showed no starting material, and di-*tert*-butylperoxide (DTBP) was added (1.2 mL of a 5–6 M solution in decane). The solution was stirred at rt for 1.5 h and concentrated to remove some of the ACN. The remaining solution was dissolved in 200 mL of EtAc and washed with 150 mL of sat. $NaHSO_3$, 100 mL of sat. $NaHCO_3$, 100 mL of brine, dried over $NaSO_4$, and concentrated. The remaining oil was purified by flash column chromatography (50% EtAc in Hex, r_f = 0.2) to produce a clear oil (1.1573 g, 65% yield). **^{1}H-NMR** (500 MHz, $CDCl_3$, δ): 4.40 (m, 1H), 4.21 (m, 1H), 4.05 (m, 4H), 3.71 (s, 3H), 2.83 (s, 1H), 1.83–1.64 (m, 4H), 1.47 (m, 18H), 0.89 (s, 9H), 0.09 (s, 3H), 0.07 (d, 3H). **^{13}C-NMR** (125 MHz, $CDCl_3$, δ): 174.30, 174.28, 83.24, 82.63, 71.78, 70.04, 68.45, 67.05, 52.14, 30.63, 29.81, 28.03, 25.76, 25.64, 18.30, −0.00, −5.05, −5.22. **^{31}P-NMR** (150 MHz, $CDCl_3$, δ): −5.11, −5.18. **HRMS ESI-MS**: 543.275 *m*/*z* $[M + H]^+$ calculated for $C_{23}H_{47}O_{10}PSi$, 543.279 found.

***tert*-Butyl (2*S*)-5-((*tert*-butoxy((*R*)-2-((*tert*-butyldimethylsilyl)oxy)-3-methoxy-3-oxopropoxy)phosphoryl)oxy)-2-(((4-nitrophenyl)sulfonyl)oxy)pentanoate (10).** **9** (0.4900 g, 0.904 mmol) was dissolved in DCM (11.5 mL) on ice (0 °C). TEA (0.24 mL, 1.72 mmol) and NsCl (0.5860 g, 2.65 mmol) were added sequentially. The reaction mixture was stirred on ice for 1 h, allowed to warm to rt, and stirred for an additional 3 h. The reaction mixture was added to a separation funnel and washed with 50 mL of sat. $NaHCO_3$, dried over Na_2SO_4, and concentrated. The crude yellow oil was purified by flash column chromatography (25 to 50% EtAc in Hex, r_f = 0.5 in 50% EtAc in Hex) to produce a yellowish oil (0.6572 g, 75% yield). **^{1}H-NMR** (500 MHz, $CDCl_3$, δ): 8.37 (d, 2H), 8.14 (d, 2H), 4.88 (m, 1H), 4.38 (m 1H), 4.19 (m, 1H), 4.07 (m, 1H), 3.97 (m, 1H), 3.72 (d, 3H), 1.93 (m, 2H), 1.73 (m, 2H), 1.46 (d, 9H), 1.38 (s, 9H), 0.88 (s, 9H), 0.09 (s, 3H), 0.07 (s, 3H). **^{13}C-NMR** (125 MHz, $CDCl_3$, δ): 171.01, 166.87, 150.78, 142.32, 129.44, 124.29, 83.60, 78.63, 71.72, 68.55, 66.04, 52.17, 29.80, 28.55, 27.81, 25.63, 18.30, −5.04, −5.24. **HRMS ESI-MS**: 1455.499 *m*/*z* $[2M + H]^+$ calculated for $C_{29}H_{50}NO_{14}PSSi$, 1455.511 found.

^{tBu}DOTAGA-3PG. 10 (0.1749 g, 0.241 mmol) was dissolved in ACN (4 mL) and then ^{tBu}DO3A[13] (0.1415 g, 0.238 mmol) and K_2CO_3 (0.1882 g, 1.36 mmol) were added. The reaction was stirred at rt overnight. The solution was vacuum filtered, rinsed with ACN, and the filtrate concentrated. The remaining residue was suspended in ether and gravity filtered into a separation funnel. 50 mL of water was added, and the water was washed with ether (3 × 40 mL). The organic phase was dried over Na_2SO_4 and concentrated. The crude oil was purified by flash column chromatography (7.5% MeOH in DCM, r_f = 0.4) to afford a brownish oil (0.0729 g, 26% yield; product showed a $\frac{1}{2}$ salt with a nosylate). **^{1}H-NMR** (500 MHz, $CDCl_3$, δ): 8.13 (d, 2H), 4.39 (m, 1H), 4.20 (m, 1H), 4.07–3.97 (m, 4H), 3.72 (s, 3H), 3.36 (m, 3H), 3.15 (m, 3H), 2.79 (m, 2H), 2.49 (m, 3H), 2.30 (m, 3H), 2.11 (m, 4H), 1.80–1.60 (m, 4H), 1.43 (m, 45H), 0.88 (s, 9H), 0.09 (s, 3H), 0.07 (s, 3H). **^{13}C-NMR** (125 MHz, $CDCl_3$, δ): 173.08, 172.97, 172.95, 171.01, 168.51, 153.82,

 This journal is © The Royal Society of Chemistry 2024

Open Access Article. Published on 25 October 2024. Downloaded on 4/21/2026 11:49:17 AM. This article is licensed under a Creative Commons Attribution-NonCommercial 3.0 Unported Licence.

147.79, 127.69, 123.11, 82.59, 82.29, 81.89, 71.67, 68.53, 66.88, 61.08, 55.91, 55.61, 52.57, 52.20, 48.50, 48.11, 47.39, 47.18, 44.58, 31.08, 29.84, 27.90, 27.85, 27.75, 25.64, 18.31, −5.02, −5.20. **HRMS ESI-MS**: 1061.619 *m*/*z* $[M + Na]^+$ calculated for $C_{29}H_{50}NO_{14}PSSi$, 1061.646 found.

***Gd-3PG*. ^{tBu}DO3A-3PG** (54.3 mg, 52.3 μmol) was dissolved in 2 mL of THF and 2 mL of 3 M LiOH for 1 h. On ice (0 °C), 10 mL of TFA with 100 μL of TIPS was slowly added and stirred for 24 h. The solution was concentrated and redissolved in water, and the pH was adjusted to 6 using 1 M NaOH. $GdCl_3{\cdot}6H_2O$ (25 mg, 67.4 μmol) was then added and the pH was adjusted to 6 over 24 h. The solution was then filtered and purified by reverse-phase HPLC on a Synergi 4 μm Polar-RP 80 Å using an isocratic flow of 0.1% FA in water (r_f = 4.957 min). The product was lyophilized down to afford a white powder (3 mg, 7% yield). **HRMS ESI-MS**: 783.100 *m*/*z* $[M - H]^-$ calculated for $C_{22}H_{35}GdN_4O_{15}P$, 783.100 found.

(2*S*)-5-((((*R*)-2-Carboxy-2-hydroxyethoxy)(hydroxy)phosphoryl)oxy)-2-hydroxy pentanoic acid (3PG-Arm). Intermediate **9** (48.9 mg, 0.090 mmol) was dissolved in 3 M LiOH (250 μL) and THF (250 μL) for 15 min, and then TFA with 5% TIPS (5 mL) was slowly added on ice (0 °C) for 1 h. The solution was concentrated, and the crude product was purified by reverse phase HPLC on an Atlantis C18 in 0.1% TFA with an isocratic flow to afford a clear liquid (15.0 mg, 55% yield). **^{1}H-NMR** (500 MHz, D_2O, *δ*): 4.49 (m, 1H), 4.32 (m, 1H), 4.15 (m, 2H), 3.92 (m, 2H), 1.90 (m, 1H), 1.75 (m, 3H). **^{13}C-NMR** (125 MHz, D_2O, *δ*): 177.71, 174.64, 69.91, 69.97, 67.25, 66.00, 29.68, 25.36. **HRMS ESI-MS**: 303.047 *m*/*z* $[M + H]^+$ calculated for $C_8H_{15}O_{10}P$, 303.050 found.

Results and discussion

Synthesis

The synthesis was designed similarly to previous albumin binding agents like MS-325, which have an arm composed of a phosphodiester with aromatic moieties.[14,15] Our work focuses on installing an arm with a common glycolytic metabolite, 3-phosphoglycerate (3PG) (Scheme 1). Commercial sources of protected *R* enantiomeric pure glyceric acid **1** are derived from the carbohydrate oxidation of mannitol.[12] A quantitative yield of compound **2** was obtained after deprotection of the acetal with Dowex 50WX8.[12] The hydroxyl groups were protected with TBS-Cl and imidazole in DMF to yield **3**.[16] A selective deprotection of the primary over the secondary TBS protected hydroxyl was carried out using acetic acid in a single liquid phase with water and acetone as cosolvents.[17] Care was taken during the workup as the acetic acid was slowly quenched with solid $NaHCO_3$ on ice to prevent further deprotection. A liquid extraction with dichloromethane and water allowed for easy separation of acetate and product **4**, which was further purified by column chromatography.

The phosphodiester formation of the 3PG-arm is similar to the work done for synthetic DNA utilizing phosphorodiamidite substitution.[18] The *tert*-butyl protected phosphorodiamidite was activated with tetrazolide and substituted with the primary hydroxyl of **4** to produce a high yield of **5**. This intermediate was used relatively quickly because of its sensitivity to oxidation or hydrolysis. **5** was substantially non-polar compared to byproducts and was easily purified on a deactivated silica plug. The primary hydroxyl of intermediate **8**[10,11] showed selective substitution over the secondary hydroxyl to yield **9**.

Table 1 The relaxivity of ***Gd-3PG*** in 1× PBS, gadoterate, and gadobutrol at 1.4 T and 7 T

GBCA	1.4 T at 37 °C (mM^{-1} s^{-1})	7 T (mM^{-1} s^{-1})
Gd-3PG	5.39 ± 0.14	5.61 ± 0.08[b]
Gadoterate[a]	3.32 ± 0.13	2.84 ± 0.08
Gadobutrol[a]	4.78 ± 0.12	3.83 ± 0.24

[a] Agents are in human plasma at 37 °C.[21] [b] At 21 °C.

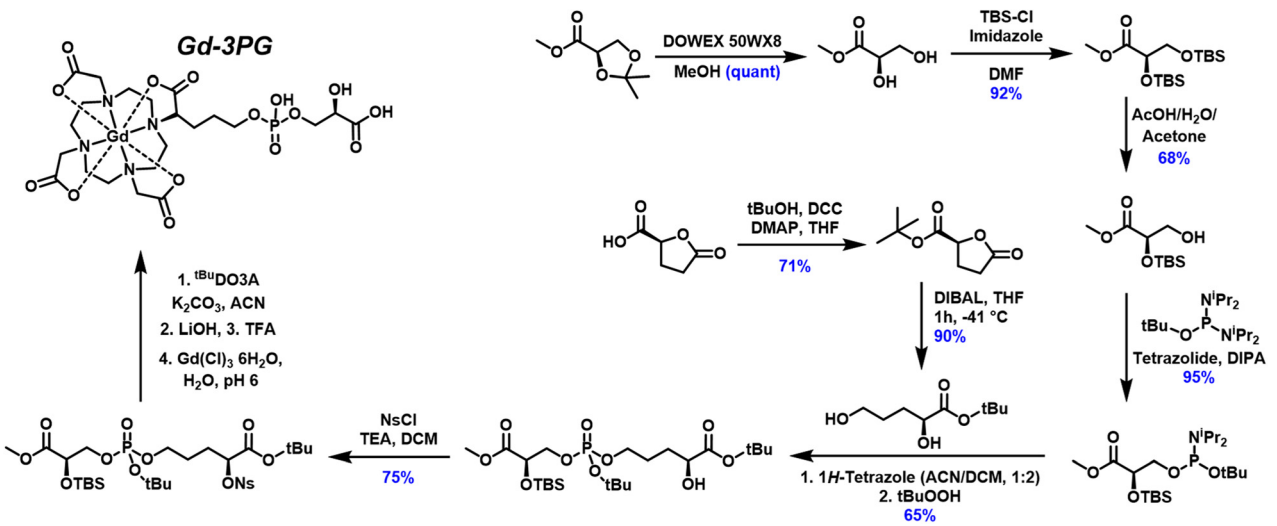

Scheme 1 Synthetic scheme for the preparation of ***Gd-3PG***.

Open Access Article. Published on 25 October 2024. Downloaded on 4/21/2026 11:49:17 AM.
This article is licensed under a Creative Commons Attribution-NonCommercial 3.0 Unported Licence.

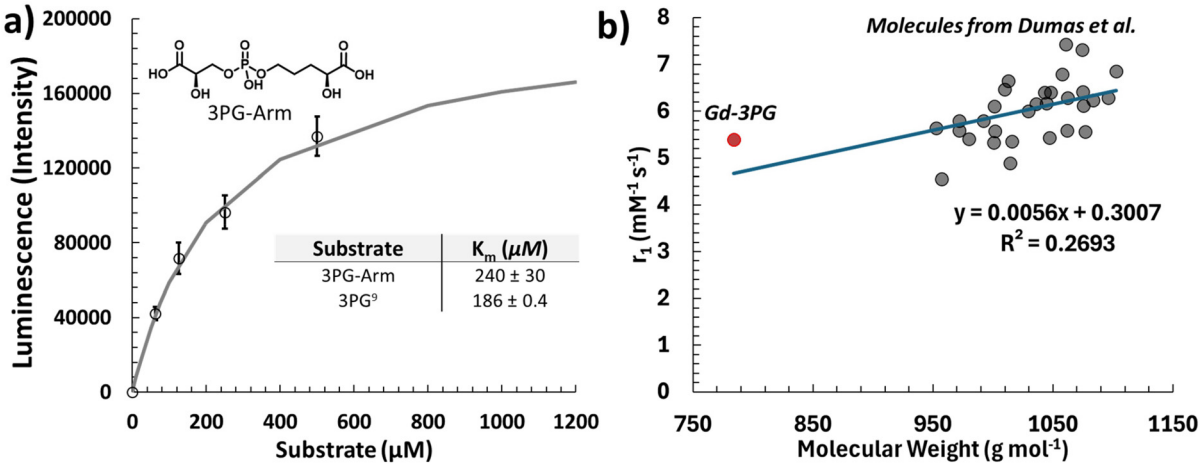

Fig. 1 (a) Michaelis–Menten plot of the 3PG-arm being phosphorylated with PGK using an ADP-Glo Kinase assay. The kinetics of 3PG to 1,3-BPG is from the literature using an assay coupled to excess GAPDH tracking the loss of NADH.[9] (b) Extrapolated plots showing the relationship between molecular weight and the r_1 of similar phosphodiester GBCAs.[14] With a relaxivity of 5.4 mM^{-1} s^{-1}, ***Gd-3PG*** is above the trendline indicating a higher secondary sphere effect. However, based on the literature values (R^2 = 0.2693), there is some uncertainty in the relationship between molecular weight and r_1.

The secondary hydroxyl was then activated with nosyl chloride, **10**, and used for an S_n2 reaction with ^{tBu}DO3A.[13] Base deprotection with LiOH/THF was used to remove the methyl ester, and the reaction was adjusted to acidic conditions with TFA and TIPS as scavengers. It is essential to perform the base deprotection before adjusting to acidic conditions as the phosphodiester has a higher rate of hydrolysis under basic conditions, especially intramolecularly.[19] The metalation was performed with $GdCl_3$ and the resulting product was purified by HPLC to yield ***Gd-3PG***. The polar endcap, phenyl ester (C18), required an isocratic method in acid buffer to retain ***Gd-3PG***. Higher substitutions of ***Gd-3PG*** would require a form of anion exchange or ion-pairing to purify similar to oligonucleotides and mononucleotides.[20]

Relaxivity measurements

r_1 measurements were taken under different magnetic fields and at different temperatures (1.4 T at 37 °C and 7 T at 21 °C). Typically, the r_1 decreases with an increase in magnetic field strength, but since the temperature is lower at 7 T, the r_1 of ***Gd-3PG*** appears the same (Table 1). The r_1 of ***Gd-3PG*** is higher than that of common gadoterate and more similar to the trend of gadobutrol. The increase in ***Gd-3PG*** could either be due to the increase in molecular weight or attributed to the secondary sphere effects of the hydrogen bonding moieties, specifically the phosphodiester, hydroxyl, and carboxylic acid groups.

Gd-3PG was then extrapolated with data from previously published phosphodiester incorporated GBCAs (Fig. 1b).[14] While ***Gd-3PG*** is above the trendline, indicating a higher secondary sphere effect, there is significant uncertainty in the relationship between molecular weight and r_1.

Enzymatic assays

Enzymatic kinetics was determined using the 3PG-Arm, which showed phosphorylation by PGK. A Michaelis–Menten constant of K_m = 240 ± 30 μM was obtained, similar to that of the known 3PG metabolite[9] (Fig. 1a). This demonstrates that even modified 3PG metabolites can be phosphorylated enzymatically. When compared to controls without PGK, ***Gd-3PG*** showed no change in r_1 under active buffer conditions with PGK (Fig. S3†). This could be due to the low influence of phosphorylation on r_1 or the decreased activity of PGK caused by the macrocyclic chelator. During these experiments, it was determined that ATP concentrations increase the r_1 for both gadoterate and ***Gd-3PG*** with similar slopes (Fig. S2†). The effect of ATP on r_1 is therefore independent of the 3PG-arm.

Conclusion

The synthesis of a GBCA conjugated to a glycolytic metabolite (3PG) is reported to afford a relatively high yield of the synthetic 3PG-arm (**10**, 29% linear yield). The r_1 of ***Gd-3PG*** was higher than that of common gadoterate due most likely to secondary sphere effects or molecular weight enhancement from the 3PG-arm (5.39 ± 0.14 mM^{-1} s^{-1} at 1.4 T and 37 °C). The 3PG-arm demonstrated enzymatic activity, showing the possibility of modifying metabolites for future MRI probes. These results demonstrate the potential to use glycolytic metabolites conjugated to GBCAs for investigating metabolic function.

Data availability

The authors confirm that the data supporting the findings of this study are available within the article and its ESI.† Raw data that support the findings of this study are available from the corresponding author, upon reasonable request.

This journal is © The Royal Society of Chemistry 2024

Open Access Article. Published on 25 October 2024. Downloaded on 4/21/2026 11:49:17 AM. This article is licensed under a Creative Commons Attribution-NonCommercial 3.0 Unported Licence.

Conflicts of interest

The authors declare no competing financial interests.

Acknowledgements

A. R. B. gratefully acknowledges the NSF Graduate Research Fellowship Grant no. DGE-2234667. This work made use of the IMSERC MS facility at Northwestern University, which has received support from the Soft and Hybrid Nanotechnology Experimental (SHyNE) Resource (NSF ECCS-2025633), the State of Illinois, and the International Institute for Nanotechnology (IIN). This work employed the facilities of the High Throughput Analysis Laboratory (HTAL, NU).

References

1 H. Li and T. J. Meade, Molecular Magnetic Resonance Imaging with Gd(III)-Based Contrast Agents: Challenges and Key Advances, *J. Am. Chem. Soc.*, 2019, **141**(43), 17025–17041.

2 J. Wahsner, E. M. Gale, A. Rodriguez-Rodriguez and P. Caravan, Chemistry of MRI Contrast Agents: Current Challenges and New Frontiers, *Chem. Rev.*, 2019, **119**(2), 957–1057.

3 J. H. Tang, H. Li, C. N. Yuan, G. Parigi, C. Luchinat and T. J. Meade, Molecular Engineering of Self-Immolative Bioresponsive MR Probes, *J. Am. Chem. Soc.*, 2023, **145**(18), 10045–10050.

4 L. M. Lilley, S. Kamper, M. Caldwell, Z. K. Chia, D. Ballweg, L. Vistain, J. Krimmel, T. A. Mills, K. MacRenaris, P. Lee, E. A. Waters and T. J. Meade, Self-Immolative Activation of beta-Galactosidase-Responsive Probes for In Vivo MR Imaging in Mouse Models, *Angew. Chem., Int. Ed.*, 2020, **59**(1), 388–394.

5 A. Merbach, L. Helm and E. Toth, *The Chemistry of Contrast Agents in Medical Magnetic Resonance Imaging*, Wiley, 2nd edn, 2013.

6 M. Judd, E. H. Abdelkader, M. Qi, J. R. Harmer, T. Huber, A. Godt, A. Savitsky, G. Otting and N. Cox, Short-range ENDOR distance measurements between Gd(iii) and trifluoromethyl labels in proteins, *Phys. Chem. Chem. Phys.*, 2022, **24**(41), 25214–25226.

7 R. E. Moellering and B. F. Cravatt, Functional Lysine Modification by an Intrinsically Reactive Primary Glycolytic Metabolite, *Science*, 2013, **341**(6145), 549–553.

8 M. Botta, Second Coordination Sphere Water Molecules and Relaxivity of Gadolinium(III) Complexes: Implications for MRI Contrast Agents, *Eur. J. Inorg. Chem.*, 2000, **3**, 399–407.

9 C. M. Jin, X. B. Zhu, H. Wu, Y. Q. Wang and X. Hu, Perturbation of Phosphoglycerate Kinase 1 Only Marginally Affects Glycolysis in Cancer Cells, *J. Biol. Chem.*, 2020, **295**(19), 6425–6446.

10 J. Garcia-Calvo, T. Torroba, V. Branas-Fresnillo, G. Perdomo, I. Cozar-Castellano, Y. H. Li, Y. M. Legrand and M. Barboiu, Manipulation of Transmembrane Transport by Synthetic K^+ Ionophore Depsipeptides and Its Implications in Glucose-Stimulated Insulin Secretion in β-Cells, *Chem. – Eur. J.*, 2019, **25**(39), 9287–9294.

11 U. Schmidt, C. Braun and H. Sutoris, Enantioselective syntheses of (R)- and (S)-hexahydropyridazine-3-carboxylic acid derivatives, *Synthesis*, 1996, **2**, 223–229.

12 N. R. Lees, L. C. Han, M. J. Byrne, J. A. Davies, A. E. Parnell, P. E. J. Moreland, J. E. M. Stach, M. W. van der Kamp, C. L. Willis and P. R. Race, An Esterase-like Lyase Catalyzes Acetate Elimination in Spirotetronate/Spirotetramate Biosynthesis, *Angew. Chem., Int. Ed.*, 2019, **58**(8), 2305–2309.

13 D. J. Mastarone, V. S. R. Harrison, A. L. Eckermann, G. Parigi, C. Luchinat and T. J. Meade, A Modular System for the Synthesis of Multiplexed Magnetic Resonance Probes, *J. Am. Chem. Soc.*, 2011, **133**(14), 5329–5337.

14 S. Dumas, V. Jacques, W. C. Sun, J. S. Troughton, J. T. Welch, J. M. Chasse, H. Schmitt-Willich and P. Caravan, High Relaxivity Magnetic Resonance Imaging Contrast Agents Part 1 Impact of Single Donor Atom Substitution on Relaxivity of Serum Albumin-Bound Gadolinium Complexes, *Invest. Radiol.*, 2010, **45**(10), 600–612.

15 P. Caravan, N. J. Cloutier, M. T. Greenfield, S. A. McDermid, S. U. Dunham, J. W. M. Bulte, J. C. Amedio, R. J. Looby, R. M. Supkowski, W. D. Horrocks, T. J. McMurry and R. B. Lauffer, The Interaction of MS-325 with Human Serum Albumin and Its Effect on Proton Relaxation Rates, *J. Am. Chem. Soc.*, 2002, **124**(12), 3152–3162.

16 M. Ikubo, A. Inoue, S. Nakamura, S. J. Jung, M. Sayama, Y. Otani, A. Uwamizu, K. Suzuki, T. Kishi, A. Shuto, J. Ishiguro, M. Okudaira, K. Kano, K. Makide, J. Aoki and T. Ohwada, Structure-Activity Relationships of Lysophosphatidylserine Analogs as Agonists of G-Protein-Coupled Receptors GPR34, P2Y10, and GPR174, *J. Med. Chem.*, 2015, **58**(10), 4204–4219.

17 A. Kawai, O. Hara, Y. Hamada and T. Shioiri, Stereoselective Synthesis of the Hydroxy Amino-Acid Moiety of AI-77-B, A Gastroprotective Substance from Bacillus-Pumilus AI-77, *Tetrahedron Lett.*, 1988, **29**(48), 6331–6334.

18 N. D. Sinha, J. Biernat, J. McManus and H. Koster, Polymer Support Iligonucleotides Synthesis. 18. Use of Beta-cyanoethyl-N,N-dialkyamino-/N-Morpholino Phosphoramidite of Deoxynucleosides for the Synthesis of DNA Fragments Simplifying Deprotection and Isolation of the Final Product, *Nucleic Acids Res.*, 1984, **12**(11), 4539–4557.

19 J. R. Cox and O. B. Ramsay, Mechanisms of Nucleophilic Substitution in Phosphate Esters, *Chem. Rev.*, 1964, **64**(4), 317–351.

20 D. R. W. Hodgson, Physicochemical Aspects of Aqueous and Nonaqueous Approaches to the Preparation of Nucleosides, Nucleotides and Phosphate Ester Mimics, in

Open Access Article. Published on 25 October 2024. Downloaded on 4/21/2026 11:49:17 AM.
This article is licensed under a Creative Commons Attribution-NonCommercial 3.0 Unported Licence.

Advances in Physical Organic Chemistry, ed. I. H. Williams and N. H. Williams, 2017, vol. 51, pp. 187–219.

21 P. Szomolanyi, M. Rohrer, T. Frenzel, I. M. Noebauer-Hohmann, G. Jost, J. Endrikat, S. Trattnig and H. Pietsch, Comparison of the Relaxivities of Macrocyclic Gadolinium-Based Contrast Agents in Human Plasma at 1.5, 3, and 7 T, and Blood at 3 T, *Invest. Radiol.*, 2019, **54**(9), 559–564.

This journal is © The Royal Society of Chemistry 2024